JOURNAL OF THE AMERICAN WATER RESOURCES ASSOCIATION

AMERICAN WATER RESOURCES ASSOCIATION

USING LIDAR DATA ANALYSIS TO ESTIMATE CHANGES IN INSOLATION UNDER LARGE-SCALE RIPARIAN DEFORESTATION[1]

Jonathan Asher Greenberg, Erin L. Hestir, David Riano, George J. Scheer, and Susan L. Ustin[2]

ABSTRACT: Riparian vegetation provides shade from insolation to stream channels. A consequence of removing vegetation may be an increase in insolation that can increase water temperatures and negatively impact ecosystem health. Although the mechanisms of riparian shading are well understood, spatially explicit, mechanistic models of shading have been limited by the data requirements of precisely describing the three-dimensional structure of a riparian corridor. Remotely acquired, high spatial resolution LiDAR data provide detailed three-dimensional vegetation structure and terrain topography over large regions. By parameterizing solar radiation models that incorporate terrain shadowing with LiDAR data, we can produce spatially explicit estimates of insolation. As a case study, we modeled the relative change in insolation on channels in the Sacramento-San Joaquin River Delta under current conditions and under a hypothesized deforested Delta using classified LiDAR, rasterized at a 1-m resolution. Our results suggest that the removal of levee vegetation could result in a 9% increase in solar radiation incident on Delta waters, and may lead to water temperature increases. General, coarse-scale channel characteristics (reach width, azimuth, levee vegetation cover, and height) only accounted for 72% of the variation in the insolation. This indicates that the detailed information derived from LiDAR data has greater explanatory power than coarser reach-scale metrics often used for insolation estimates.

(KEY TERMS: LiDAR; riparian deforestation; riparian shade; solar irradiation model; Sacramento-San Joaquin River Delta; remote sensing; levees.)

Greenberg, Jonathan Asher, Erin L. Hestir, David Riano, George J. Scheer, and Susan L. Ustin, 2012. Using LiDAR Data Analysis to Estimate Changes in Insolation Under Large-Scale Riparian Deforestation. *Journal of the American Water Resources Association* (JAWRA) 1-10. DOI: 10.1111/j.1752-1688.2012.00664.x

INTRODUCTION

Riparian vegetation is critical to controlling the radiation environment in stream ecosystems by providing shade from solar radiation, thus moderating maximum water temperatures (Blann *et al.*, 2002; Welty *et al.*, 2002; Moore *et al.*, 2005a; Webb *et al.*, 2008). Removal of vegetation from riparian corridors is associated with a subsequent increase in water temperature (Broadmeadow and Nisbet, 2004; Moore *et al.*, 2005a). Increased water temperature can cause

[1]Paper No. JAWRA-10-0122-P of the *Journal of the American Water Resources Association* (JAWRA). Received July 27, 2010; accepted February 29, 2012.

[2]Respectively, Assistant Professor (Greenberg), Department of Geography and Geographic Information Science, University of Illinois at Urbana-Champaign, Room 220 Davenport Hall, 607 South Mathews Avenue, Urbana, Illinois 61801; Post-doctoral Research Fellow (Hestir), Center for Spatial Technologies and Remote Sensing (CSTARS), Land, Air and Water Resources, University of California, Davis, California 95616, and Post-doctoral Research Fellow, Environmental Earth Observation, Division of Land and Water, Commonwealth Scientific and Industrial Research Organization (CSIRO), Australia; Project Scientist (Riano), Research Technician (Scheer), and Professor of Environmental Resource Science (Ustin), Center for Spatial Technologies and Remote Sensing (CSTARS), Land, Air and Water Resources, University of California, Davis, California 95616 (E-Mail/Greenberg: jgrn@illinois.edu).

changes to fish habitat, behavior, and overall health, shifts in species abundance and distribution, changes in production, algal blooms, and different water chemistry (Marsh *et al.*, 2005). The mechanisms of riparian shading and the impacts of its removal on water temperatures have been recognized for more than 30 years, and are well understood (Webb *et al.*, 2008). However, watershed-scale stream temperature models that incorporate shade from riparian corridors have only recently come into use as technologies to address the complex and computationally intensive requirements of shading effects (Chen *et al.*, 1998b).

Mechanistic radiation models that derive instantaneous or time-integrated estimates of insolation by incorporating riparian vegetation structure necessarily employ ray-tracing algorithms. Ray-tracing algorithms simulate the path of light rays as they move within the environment. This requires precise knowledge of the location (in three dimensions) of all objects that can absorb or scatter the incident radiation. In the context of modeling the radiation environment along riparian corridors, this amounts to requiring, minimally, a dataset of the size, shape, and position of every object that can potentially intercept incoming solar radiation on the stream surface. This sampling requirement, if using field techniques, effectively precludes large-scale application of mechanistic radiation models. Remote sensing provides synoptic reach to watershed-scale datasets that can be used to effectively characterize riparian corridors without the need for interpolation or intensive field sampling. Although some studies have used remote-sensing-derived vegetation cover products in their shade models (Chen *et al.*, 1998b), vegetation cover is represented by large-scale polygons that are characterized in terms of width, average height, and average density. Thus, these approaches provide an *average* shade estimate for a selected transect of vegetation that is similar to field-based methods, which provide a channel-scale estimate of shade cast by vegetation rather than directly assessing shading on the river surface (Clark *et al.*, 2008). Other approaches to characterizing riparian shading rely on more empirical or subsampling techniques, for example, through the use of point measurements from clinometers, convex mirrors, hemispherical photography, or light meters (Moore *et al.*, 2005a). Given the complexity of the canopy/terrain/sun angle characteristics along a riparian channel, these techniques are, at best, rough estimates of the true radiation environment (e.g., Rutherford *et al.*, 1997; Moore *et al.*, 2005b). Furthermore, making the appropriate number of measurements to adequately characterize riparian environments at large spatial scales (i.e., the watershed scale) is logistically infeasible.

Remotely acquired, high spatial resolution, multiple-return LiDAR data provide the information necessary to parameterize the shade component on the river surface for a mechanistic solar radiation model across a large riparian system. LiDAR data are obtained by active sensor systems that both emit and measure laser light, determining the time since the laser pulse was emitted to calculate the distance-from-sensor (given the speed of light is a constant). By combining the distance-from-sensor, the angle of the laser pulse, and on-board inertial navigation (which includes GPS coordinates), each pulse return is placed in three-dimensional space. Objects that are not optically opaque, such as vegetation, will frequently have multiple returns per grid cell, as the laser pulse is intercepted by leaves and branches at varying heights through the canopy as well as the ground. The returned LiDAR point cloud can be converted to rasterized digital elevation models (DEMs) to produce a gridded representation of the elevation at the top of the canopy ("first return") and the ground ("bare earth") (Figure 1). As the LiDAR pulse is typically in the near-infrared (NIR) wavelengths, pulses that are incident on water will be absorbed by

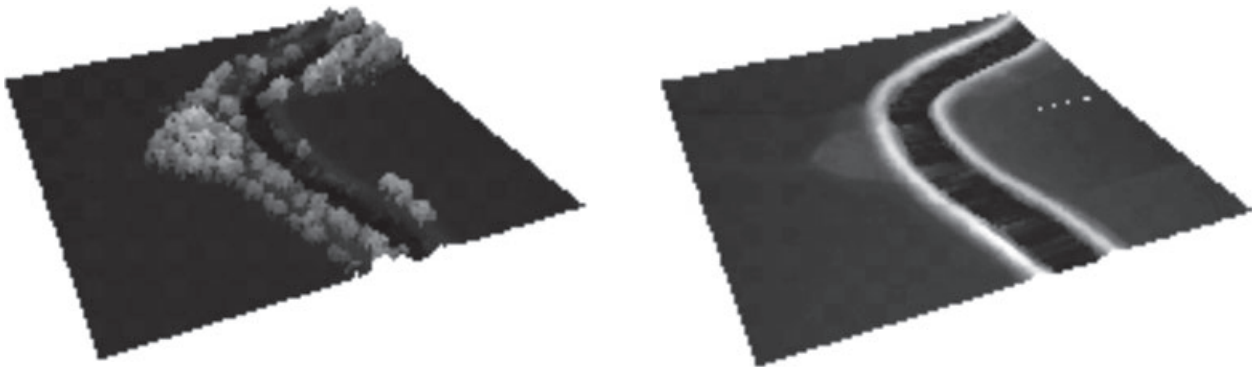

FIGURE 1. Left: LiDAR First Return Raster of a Wooded River Bend with Trees (current conditions); Right: Bare Earth Raster of the Same River Bend (treeless Delta). The images are 500 m × 500 m. Brighter values indicate higher elevation.

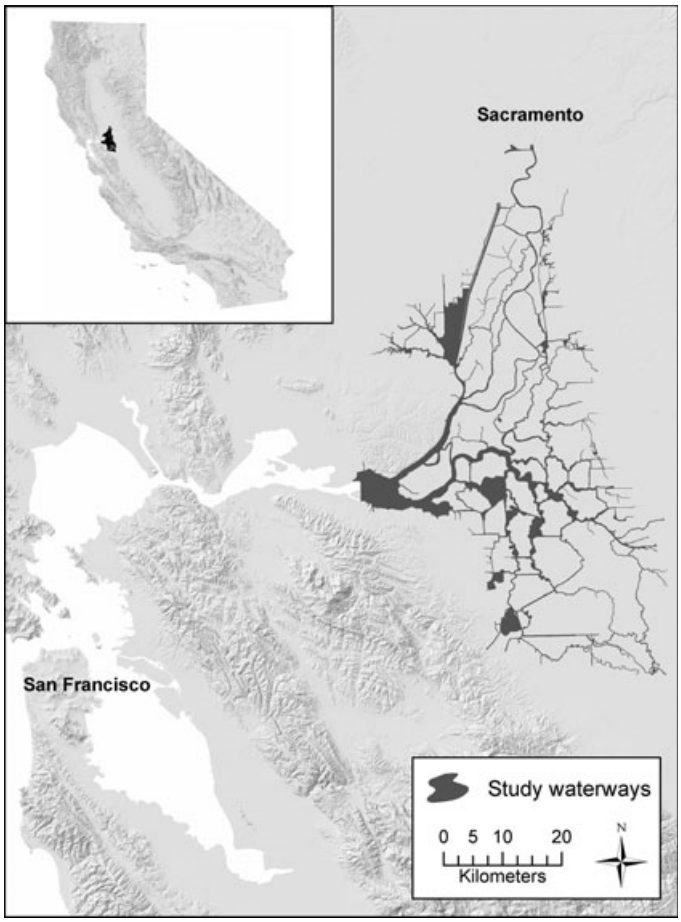

FIGURE 2. The Sacramento-San Joaquin River Delta, California.

the water column and will not return to the sensor, often leaving water bodies as no-data zones.

The objective of this study was to determine the usefulness of remote-sensing LiDAR data to resolve shade parameterization in solar radiation modeling. To this end, we selected a case study wherein riparian vegetation razing is imminent. We examined the impacts of large-scale vegetation removal on insolation of the waters of the Sacramento-San Joaquin River Delta (hereafter "the Delta"), an extensive network of over 22,000 ha of rivers, lakes, and wetlands that drain into the San Francisco Bay (Figure 2). Much of the dry land in the Delta has been subsiding, and its islands (reclaimed land tracts surrounded by Delta channels) currently range from 3 to 8 m below sea level (Ingebritsen, 2000). These islands are protected by approximately 1,800 km of levees (Lund, 2007), which are structurally unstable due to the hydraulic pressure between the subsided land and the higher water level (Mount and Twiss, 2005). For California to receive federal assistance to rehabilitate the Delta's fragile levee system, the levees must meet certain criteria, including the U.S. Army Corps of Engineers no-vegetation standard for levees (U.S. Army Corps of Engineers, 2009). This would require the removal of all riparian vegetation with stems >5 cm in diameter, including native riparian and ornamental trees, herbs, and shrubs currently growing on the levees. The most common tree species are valley oak (*Quercus lobata*), cottonwood (*Populus fremontii*), California sycamore (*Platanus racemosa*), boxelder (*Acer negundo*), willow (*Salix spp.*), and the endangered native walnut (*Juglans hindsii*). Other dominant vegetation species include Himalayan blackberry (*Rubus ameniacus*), wild rose (*Rosa californica*), stinging nettle (*Urtica dioica*), giant reed (*Arundo donax*), and a large variety of introduced grasses. However, vegetation-razing requirements have met with opposition from a number of stakeholders in the region. In response to this controversy, recent recommendations made by a group of federal, state, and local agencies include scientific research to determine whether and where vegetation removal would improve levee performance (Central Valley Flood Protection Board, 2009). However, there are other critical ecosystem impacts from vegetation removal not considered by current planning, such as the impact on water surface insolation and subsequent effects on aquatic ecosystems.

Herein, we ask: what is the maximum potential increase in insolation on Delta waters that will result from levee vegetation removal? We address these questions using a ray-tracing solar irradiation model applied to spatially explicit maps of the three-dimensional structure of the current vegetation cover and a hypothesized unvegetated Delta derived from remotely sensed LiDAR data. Additionally, we ask: what impact do reach-level spatial and vegetation properties (channel width and azimuth, vegetation cover, and mean vegetation height) have on changes in insolation?

METHODS

Input Datasets

LiDAR. The Airborne 1 Corporation acquired LiDAR data for the California Department of Water Resources (DWR) during late January to February 2007. The data were collected using an Optech ALTM-3100 on a helicopter flying at approximately 1,700 m above the terrain at a speed of approximately 120 knots. At a pulse rate of 70 kHz, the mean point density of the data was 0.787 points/m^2. The scan angle was 12°, resulting in a swath width of approximately 700 m with a 40% overlap. The reported vertical accuracy was 95% at 18.5 cm and 90% at 15 cm, and the horizontal accuracy was

30 cm. Point cloud classification was performed by Fugro EarthData, Inc. into bare earth and first return. When no vegetation was present, the bare earth and first return were equivalent. We created 1 square meter rasters of the first return and last return images using TerraScan (Soininen, 2004) software, retrieving for each 1 m^2 cell the minimum height (bare earth point elevation) and maximum height (first return point elevation). The NIR light emitted by the sensor is almost entirely absorbed by water, so regions with surface water had no recorded return, and therefore yielded a no-data value. We filled in these no-data cells by calculating the mean annual water stage for the 2007 water year (1 October 2006 to 30 September 2007) and inserting this value into the no-data locations. Water stage is measured by an extensive network of water height gages and freely available for download from the California DWR California Data Exchange Center (Department of Water Resources, 2009).

Radiation Calculations

There are many solar radiation models available for use, and a review of several models' properties and performance is described in Ruiz-Arias *et al.* (2009). We used the r.sun model (Hofierka and Šúri, 2002) running within the GRASS GIS environment (GRASS Development Team, 2009) to calculate per-pixel insolation for all waterways. The r.sun model calculates direct (beam) and diffuse radiation at every grid cell in a raster map under real sky (overcast) or clear-sky (cloudless) conditions. This model can incorporate sky obstruction using line-of-sight shadowing in addition to solar angle/ground angle calculations, which makes it ideal for directly assessing the location and amount of shade created by every plant detected in the LiDAR dataset.

We applied the r.sun model to the bare earth and first return LiDAR DEMs. The model integrated the daily solar irradiation, calculated using 30-min intervals for three summer dates: 29 June, 29 July, and 28 August. We ran the model using clear-sky (cloud-free) conditions typical of summers in central California with a Linke atmospheric turbidity factor of 3.0, a typical average value for clear-sky conditions in rural-city areas (Šúri and Hofierka, 2004). Daily summer irradiation was calculated as the average daily irradiation for the three dates. As we were interested in insolation at the surface of the water, in regions which had multiple returns (e.g., vegetation) we assumed the direct component of the radiation environment under the vegetation to be 0 $Wh/m^2/day$, rather than the modeled radiation at the top of the plant canopy.

Due to the size of the input LiDAR surfaces (approximately 36 GB each), we ran the algorithm in 1,200 m × 1,200 m tiles, in which each adjacent tile overlapped by 100 m on each side. The central 1,000 m × 1,000 m outputs from each tile were stored and, once all the tiles were processed, merged back into a single output image.

Model Validation

Solar irradiance modeling under clear-sky conditions is essentially a geometry problem combined with a ray-tracing problem. Although we did not directly validate the irradiance estimates using point-based estimates, Šúri *et al.* (2005) found that r.sun estimates for all of Europe had a mean RMSE compared with meteorological station measurements of solar radiation of 5.2%, demonstrating the accuracy of the sun angle/-ground angle portion of the model. A different study comparing various solar irradiance models found r.sun had an RMSE *vs.* clear-sky ground measurements of 2.35%, among the best of all models studied (Ruiz-Arias *et al.*, 2009). As the objective of our analysis was to evaluate the LiDAR data for parameterization for precise shadowing estimates, we did validate the shadowing portion of the algorithm by running r.sun for time periods that coincide with the acquisition of two aerial remote-sensing images collected at 3-m ground resolution using the HyMap imaging spectrometer (HyVista Corporation, Castle Hill, NSW, Australia) on June 21 and 22 2007 around 16:30 UTC. Points were randomly chosen within a waterways polygon coverage of the Delta (Hestir *et al.*, 2008) (n = 78) stratified by regions where there was predicted to be shadow at that time period (n = 40), and where there should not be shadows (n = 38). Each of these random points was identified as "shadow" or "not shadow" in a three-band true-color composite by photointerpretation. By comparing the estimated shadow and not-shadow maps with the photointerpreted points, we calculated a confusion matrix and accuracy statistics.

Data Extraction and Summarization

In order to summarize our calculations of maximum insolation into a relevant management scale, we summarized the 1-m^2 grid cell insolation values by river reach. We defined river reaches using the Delta waterways coverage described in Hestir *et al.* (2008), subdivided into individual channels. We aggregated all reaches shorter than 500 m in length into their parent channel. We then created a line network of Delta channels from the center of each individual channel polygon.

We calculated the insolation change between the current and vegetation-less Delta maps at local (each 1-m^2 grid cell), individual reach, and Delta-wide scales. The local-scale mean, minimum, and maximum insolation and the insolation changes (first return – bare earth) were calculated directly using the ray tracing model output rasters. The zonal statistics (mean, minimum, maximum, and change in the local surface irradiation) for each reach were extracted from the output rasters using the vector-raster program STARSpan (Rueda *et al.*, 2005).

Reach Spatial and Vegetation Properties Effect on Insolation Changes

To determine whether the insolation change under vegetation razing is an effect of general channel spatial or vegetation properties as opposed to small-scale, spatially explicit properties, we conducted a regression analysis to determine the amount of variability in insolation that the coarse-scale properties explain. To obtain the predictor variables, we calculated the reach width, azimuth, levee vegetation cover, and mean levee vegetation height. Reach width was estimated by calculating the mean distance between each location along the Delta line network and the closest shoreline. These locations were averaged for each reach polygon. Reach azimuth was estimated by calculating the mean azimuth for each location along the Delta line network and summarizing by each reach polygon. To quantify the degree to which a reach runs north-south *vs.* east-west, azimuths were transformed to a single quadrant measurement between 0 (the channel runs north-south) and 90 (the channel runs east-west).

We estimated channel vegetation properties by calculating a 100-m buffer around each reach polygon, and extracting the LiDAR data from these locations. Vegetation cover was based on the amount of area in which LiDAR heights (the difference between the first return and bare earth elevations) were >0.25 m as a fraction of the total terrestrial area within the 100-m buffer. Vegetation height per reach was calculated as the mean vegetation height of all locations within the 100-m buffer.

We ran a multiple linear regression (MLR) model using the R statistical analysis software (R Development Core Team, 2011) regressing the change in insolation for each reach polygon as a function of channel width, azimuth, vegetation cover, and vegetation height. We used forward selection and backward elimination in a standard stepwise regression to select significant predictor variables and the Akiake's information criterion (AIC) for model specification (Gotelli and Ellison, 2004).

FIGURE 3. True-Color Subset of a Validation Aerial Image (HyMap) with the Boundaries of r.sun Modeled Shadows for the Same Date and Time as the Aerial Overflight Outlined in Yellow. The actual shadows can be seen projecting roughly west from the shoreline. Pixel sizes are 3 m.

RESULTS

Shadow Validation

Comparison between the modeled shadow positions and photointerpreted shadow positions from the HyMap imagery yielded an overall accuracy of 92% (see Figure 3). The errors in shadowing fell into one of four categories: (1) underestimates of the area of the modeled shadows likely due to the LiDAR pulses not being intercepted by the leaves at the edge of crown, (2) small geographic misregistration errors between the LiDAR data and the aerial photography, (3) shadows caused by riparian vegetation that was present during the LiDAR acquisition but was no longer present when the aerial photography was acquired approximately 6 months later, and (4) an inability to visually identify shadows from small plants in the 3-m imagery.

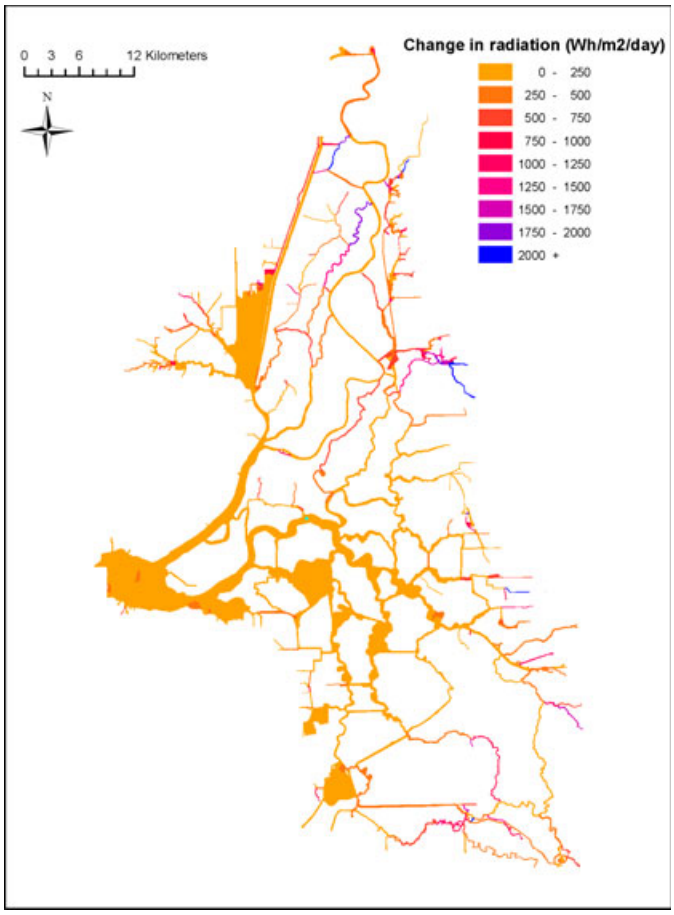

FIGURE 4. Change in Solar Radiation Under Riparian Deforestation for Individual Reaches.

Estimates of Changes in Solar Irradiance Under Vegetated and Unvegetated Conditions

Delta-wide, we estimated that by removing vegetation the daily summer irradiation incident on the water surface would increase by 9%, from 7,430 to 8,077 Wh/m^2/day. At the reach scale, irradiation on the water was estimated to range from 216 to 8,150 Wh/m^2/day under current conditions, increasing to 7,048 to 8,150 Wh/m^2/day under an unvegetated Delta. At a local (1 m^2) scale, irradiation on the water surface was estimated to range from 0 to 8,321 Wh/m^2/day under current conditions and 516 to 8,445 Wh/m^2/day under a vegetation-less Delta (Figures 4 and 5). The minimum irradiation increasing from 0 Wh/m^2/day (current conditions) to 516 Wh/m^2/day (vegetation-less conditions) was due to the terrain alone providing no all-day shadowing anywhere in the Delta.

TABLE 1. Significant Regression Coefficients (significance considered at $p < 0.01$) and Standard Errors in Multiple Linear Regression.

Coefficient	Estimate	Standard Error	*P*
Intercept	131.01	19.58	<0.01
Reach width	−0.88	0.28	<0.01
Vegetation cover	−246.91	70.31	<0.01
Vegetation height	361.22	11.84	<0.01

Note: Coefficient and model selection determined from stepwise regression and AIC.

Reach Spatial and Vegetation Property Effect on Change

The mean width of reaches was 59.72 m (SD = 37.17), ranging from 2.0 to 576.6 m. Their mean azimuth was 56.01° (SD = 14.55), ranging from 0° to 90°. The mean vegetation cover within 100 m of the shoreline was 25.2% (SD = 21.2), ranging from 0% to 100% cover. Mean vegetation height within the 100-m buffer was 0.77 m (SD = 1.19), ranging from 0.00 to 7.30 m.

Of the four predictors, three were found to be significant in predicting the change in vegetation: channel width, existing vegetation cover, and mean vegetation height (Table 1). Channel azimuth did not

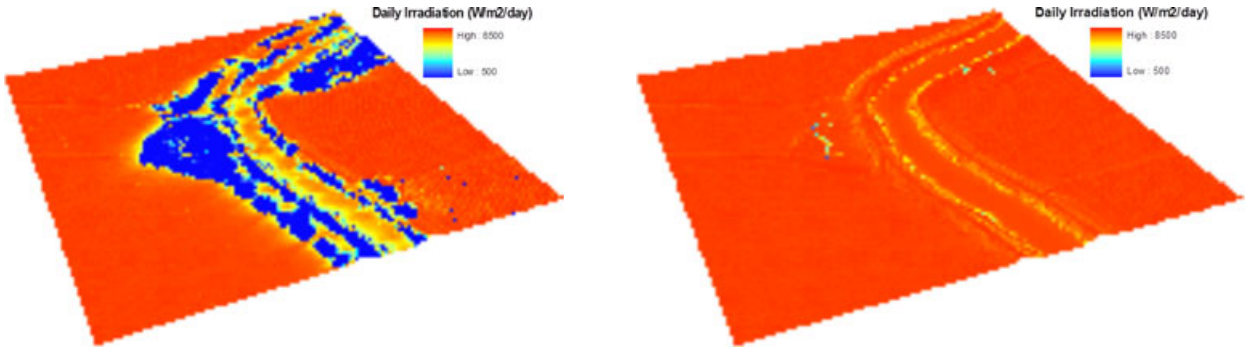

FIGURE 5. Left: Solar Radiation of a Wooded River Bend with Trees (current conditions); Right: Solar Radiation If Trees Are Removed (treeless Delta). The images are 500 m × 500 m.

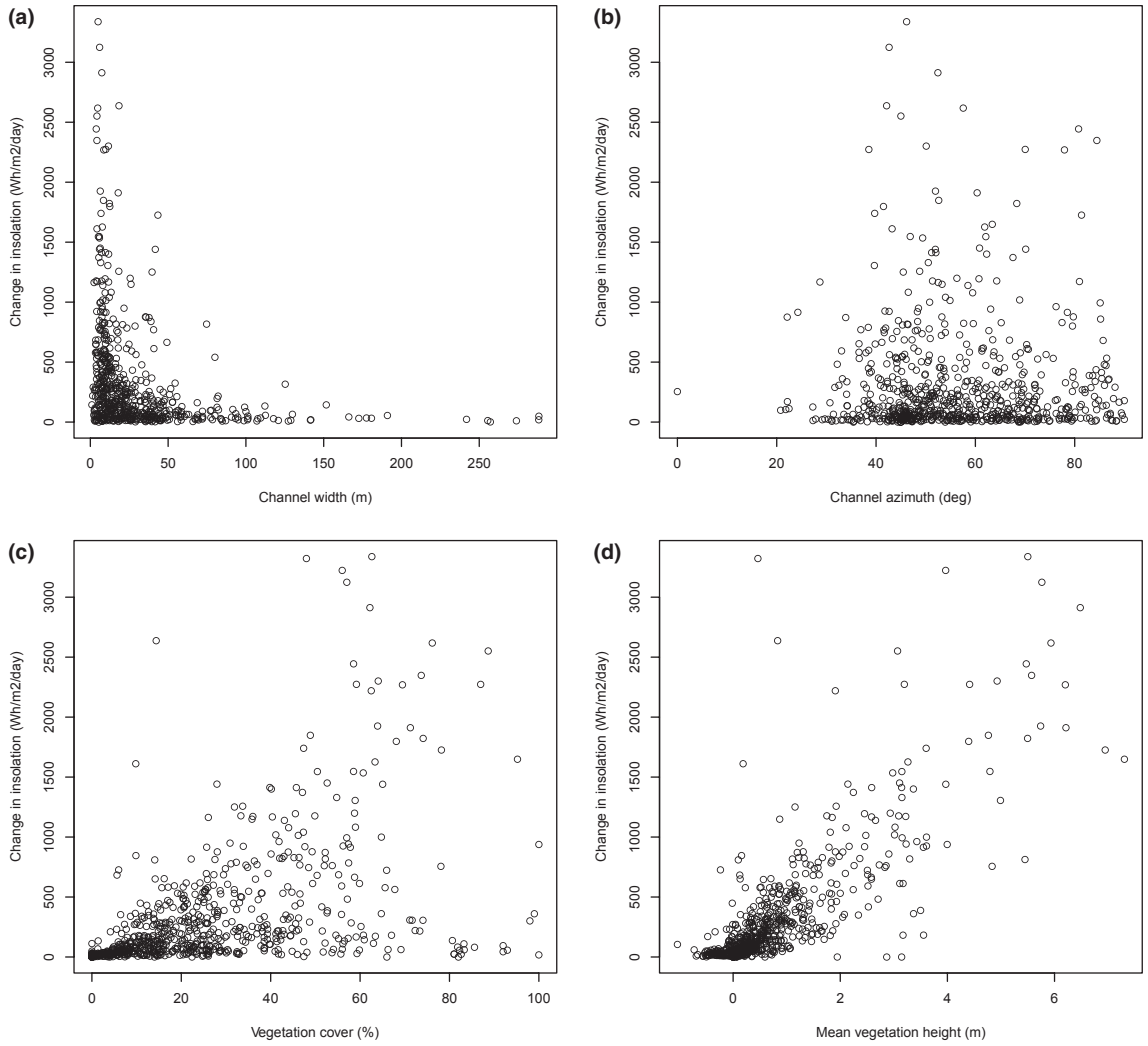

FIGURE 6. Changes in Insolation as a Function of Channel Characteristics: (a) Channel Width, (b) Channel Azimuth, (c) Vegetation Cover (100 m buffer from the shore), and (d) Mean Vegetation Height (100 m buffer from the shore).

have a significant effect on the estimated change in insolation between current and unvegetated conditions ($p = 0.31$). There were no substantial changes in model performance (AIC ranged from 6,907.28 to 6,908.26). The final MLR model selected had a multiple $R^2 = 0.7205$ and an adjusted $R^2 = 0.7192$; the adjusted R^2 did not vary from other models. The final partial regression coefficient estimates are summarized in Table 1. See Figure 6 for scatterplots of these predictors *vs.* the change in insolation.

DISCUSSION

Current riparian vegetation shading of the Delta reduces insolation by an average of 647 Wh/m^2/day during summer under clear-sky conditions. Removal of vegetation from levees in the Delta would result in a spatially variable increase in solar radiation. Thus, the results from the MLR of reach characteristics against change in radiation are unsurprising. Vegetation cover and height are indicative of vegetation presence, thus their partial regression coefficients have the greatest contribution. Overall, the results from the MLR demonstrated that wider reaches with little or low stature existing riparian vegetation would see little impact from levee vegetation removal, whereas narrower channels with considerable, tall riparian vegetation will see the biggest impacts. The benefit of a detailed high-resolution LiDAR approach to estimating insolation can be seen through the results of the MLR model: the coarse-scale reach predictors (channel width, vegetation cover and height, and channel direction) we identified explain only 72% of the variation in insolation changes under the vegetation-razing scenario. Field-based or coarse remote sensing-based approaches typically use similar reach-

scale estimates for shading such as vegetation cover and height. Yet, 28% of the change in insolation we modeled could not be explained by these coarser variables. LiDAR data provide the spatially explicit information needed to better characterize shading for solar radiation models without the need to approximate cover through coarser, less explanatory variables.

We applied our model result to a simple temperature model in order to provide a first-order estimate of the impact on water temperatures (Greenberg *et al.*, 2008). Following Halliday and Resnick (1988), we estimated the change in temperature with the additional radiation under treeless conditions as:

$$\frac{(T_f - T_i)}{\tau} = \frac{(S_f - S_i)A}{dcV},$$

where ($T_f - T_i$, °C) is the estimated change in temperature between the current (i) conditions and the treeless (f) conditions over the course of a day (τ) for a column of water. ($S_f - S_i$) is the estimated change in daily irradiation between current and treeless conditions (Wh/m^2/day), A is the surface area of the water column (in our case, the resolution of the Lidar image, or 1 m^2), d is the density of water (assumed to be 1,000 kg/m^3), c is the specific heat capacity of water (4,190 J/kg), and V is the volume of the water column (m^3). V was estimated as the product of the surface area of the water column (1 m^2) and the difference between the annual average stage height of the water for the 2007 water year for all stations in the Delta (1.27 m above sea level, a.s.l.) and the bathymetric elevation. We simplified the assumptions such that: (1) all radiation is absorbed by the water column and is converted to heat energy, (2) there is no heat flow into or out of the local water column (advection is discounted), and (3) there is no reradiation. Delta-wide, we estimate a 0.1°C increase in water temperature should the trees be removed, with individual channels warming by as much as 3.9°C. These changes were estimated to result in a 0°C to 14.3°C change in water temperature at a local scale.

Although consistent with other publications on the effect of riparian shading (e.g., Rutherford *et al.*, 1997; Chen *et al.*, 1998b; Ebersole *et al.*, 2003; Davies-Colley and Rutherford, 2005), the estimates from this study are for maximum potential changes in insolation, and are thus toward the higher range of insolation changes likely to be found should vegetation be removed. Our assumptions in developing this model naturally resulted in liberal estimates of change. First, the model assumes clear-sky conditions. Although cloud-free days occur frequently in the Delta during the summer months, any presence of clouds or increased atmospheric turbidity will reduce atmospheric transmission of irradiance, and increase the relative ratio of diffuse to beam irradiance. By incorporating cloud information from, for instance, GOES satellite data, we can provide more realistic estimates of incident radiation, broken into direct and diffuse components. Second, we treat riparian vegetation as opaque objects, precluding any beam irradiance. Trees and shrubs are not optically opaque, and direct transmission of light occurs through gaps in the canopy, as well as through the leaves themselves. A better model of plant canopy light transmission taking into consideration, minimally, a canopy's leaf area index and leaf angle distribution, would increase the accuracy of these estimates (e.g., Riaño *et al.*, 2004; Widlowski *et al.*, 2007). Finally, we have considered insolation only: we have modeled incident solar (shortwave) radiation, but not longwave radiation emitted from vegetation itself that can contribute to the total amount of radiation a stream receives (Chen *et al.*, 1998a). However, under clear-sky conditions, the shading effects on shortwave beam irradiation are likely the dominant component of stream radiation environments and increases in longwave radiation from vegetation presence are offset by decreased shortwave diffuse and atmospheric longwave radiation (Dewalle, 2008).

Our primary objective for this study was to determine the usefulness of LiDAR data for parameterizing the shaded component of solar radiation models. Although an improved solar radiation model could improve the estimates of incident radiation on Delta water surfaces, our results show that the removal of vegetation will lead to an increase in insolation through a loss of shading. These results imply that vegetation-removal plans could negatively affect aquatic ecology, and that this effect is likely to occur in some critical fish habitats in the Delta. The channels that will see some of the largest impacts are also sites that are increasingly recognized as important habitat for rearing Chinook and Steelhead salmon (Moyle, 2002), two native groups of fish that are of concern to resource managers. Specifically, narrow river channels in the Northern Delta, such as Steamboat Slough, could experience an increase in insolation up to 1,414 Wh/m^2/day, and southern river channels such as Middle and Old Rivers could increase by 777 Wh/m^2/day and 1,330 Wh/m^2/day. This increase in insolation may result in increasing already high water temperatures, contributing to egg, larval, and fry mortality (Myrick and Cech, 2004).

CONCLUSIONS

The use of small-footprint LiDAR first return data in a ray-trace model allows us to directly assess the shade

present in any desired location at resolutions relevant to the impacts of individual plants. In a management scenario such as the case of the Delta, where specific locations and indeed specific trees may be identified for removal, this scale of analysis is critical to informing the secondary consequences of such decisions. Recognizing the limitations on the model, we contend that LiDAR data provide improvements for parameterizing a system-wide model of the impacts of riparian corridors on solar insolation. Incorporating a LiDAR-shading model into a stream radiation model *sensu* Dewalle (2008) would provide a complete estimate of the total radiation environment incident on Delta waters. Finally, such an analysis can be directly embedded into spatially explicit models of water temperature (e.g., Chen *et al.*, 1998a,b), to provide a detailed assessment of seasonal and diurnal water temperature changes and subsequent ecological impacts.

The final potential of this approach to modeling solar irradiation is that it cannot only be used to examine the impacts of vegetation removal, but also to address restoration impacts in a relatively straightforward fashion. Plants can simply be simulated and "pasted" into the first return raster. The shading effects from vegetation of different heights, planted in different locations along the levees, can be simulated in order to inform restoration efforts by providing guidance as to where will be the most effective gain of shade.

ACKNOWLEDGMENTS

We thank the University Affiliated Research Center (UARC) in cooperation with the Earth Sciences Division, NASA Ames Research Center and the Interagency Ecological Program for funding, and the California Department of Water Resources for providing the LiDAR for this project. In addition, we would like to thank Jessica Gorin, Maria Santos, and BDC for providing support for this project.

LITERATURE CITED

Blann, K., J.F. Nerbonne, and B. Vondracek, 2002. Relationship of Riparian Buffer Type to Water Temperature in the Driftless Area Ecoregion of Minnesota. North American Journal of Fisheries Management 22:441-451.

Broadmeadow, S. and T.R. Nisbet, 2004. The Effects of Riparian Forest Management on the Freshwater Environment: A Literature Review of Best Management Practice. Hydrology and Earth System Sciences 8:286-305.

Central Valley Flood Protection Board, 2009. California's Central Valley Flood System Improvement Framework. Central Valley Flood Protection Board , Sacramento, California.

Chen, Y.D., R.F. Carsel, S.C. McCutcheon, and W.L. Nutter, 1998a. Stream Temperature Simulation of Forested Riparian Areas: I. Watershed-Scale Model Development. Journal of Environmental Engineering 124:304-315.

Chen, Y.D., S.C. McCutcheon, D.J. Norton, and W.L. Nutter, 1998b. Stream Temperature Simulation of Forested Riparian Areas: II. Model Application. Journal of Environmental Engineering 124:316-328.

Clark, P.E., D.E. Johnson, and S.P. Hardegree, 2008. A Direct Approach for Quantifying Stream Shading. Rangeland Ecology & Management 61:339-345.

Davies-Colley, R.J. and J.C. Rutherford, 2005. Some Approaches for Measuring and Modelling Riparian Shade. Ecological Engineering 24:525-530.

Department of Water Resources, 2009. California Data Exchange Center. http://cdec.water.ca.gov.

Dewalle, D.R., 2008. Guidelines for Riparian Vegetative Shade Restoration Based Upon a Theoretical Shaded-Stream Model. Journal of the American Water Resources Association 44(6):1373-1387.

Ebersole, J.L., W.J. Liss, and C.A. Frissell, 2003. Cold Water Patches in Warm Streams: Physicochemical Characteristics and the Influence of Shading. Journal of the American Water Resources Association 39:355-368.

Gotelli, N. and A. Ellison, 2004. A Primer of Ecological Statistics. Sinauer Associates, Sunderland, Massachusetts, 510 pp.

GRASS Development Team, 2009. Geographic Resources Analysis Support System (GRASS) Software v. 6.4. Open Source Geospatial Foundation. http://grass.osgeo.org.

Greenberg, J.A., E.L. Hestir, and S.L. Ustin, 2008. The Impacts of Riparian Tree Removal on Water Temperatures in the Sacramento-San Joaquin River Delta Using LiDAR Data Analysis. American Geophysical Union, Fall Meeting 2008, San Francisco, California.

Halliday, D. and R. Resnick, 1988. Fundamentals of Physics. John Wiley & Sons, Inc., New York.

Hestir, E.L., S. Khanna, M.E. Andrew, M.J. Santos, J.H. Viers, J.A. Greenberg, S.S. Rajapakse, and S.L. Ustin, 2008. Identification of Invasive Vegetation Using Hyperspectral Remote Sensing in the California Delta Ecosystem. Remote Sensing of Environment 112:4034-4047.

Hofierka, J. and M. Šúri, 2002. The Solar Radiation Model for Open Source GIS: Implementation and Applications. Proceedings of Open Source GIS-GRASS Users Conference, Trento, Italy.

Ingebritsen, S.E., 2000. Delta Subsidence in California: The Sinking Heart of the State. U.S. Department of the Interior, U.S. Geological Survey, USGS report FS-005-00. http://pubs.usgs.gov/fs/2000/fs00500/pdf/fs00500.pdf.

Lund, J.R., 2007. Envisioning Futures for the Sacramento-San Joaquin Delta. Public Policy Institute of California, San Francisco, California.

Marsh, N., C. Rutherford, and S. Bunn, 2005. The Role of Riparian Vegetation in Controlling Stream Temperature in a South-East Queensland Stream. CRC for Catchment Hydrology Technical Report 5.

Moore, R., D.L. Spittlehouse, and A. Story, 2005a. Riparian Microclimate and Stream Temperature Response to Forest Harvesting: A Review. Journal of the American Water Resources Association 41:813-834.

Moore, R.D., P. Sutherland, T. Gomi, and A. Dhakal, 2005b. Thermal Regime of a Headwater Stream Within a Clear-Cut, Coastal British Columbia, Canada. Hydrological Processes 19(13):2591-2608.

Mount, J. and R. Twiss, 2005. Subsidence, Sea Level Rise, and Seismicity in the Sacramento-San Joaquin Delta. San Francisco Estuary and Watershed Science 3:5.

Moyle, P., 2002. Inland Fishes of California. University of California Press, Berkeley, California.

Myrick, C.A. and J.J. Cech, 2004. Temperature Effects on Juvenile Anadromous Salmonids in California's Central Valley: What Don't We Know? Reviews in Fish Biology and Fisheries 14:113-123.

R Development Core Team, 2011. R: A Language and Environment for Statistical Computing. R Foundation for Statistical

Computing, Vienna, Austria, ISBN: 3-900051-07-0. http://www.R-project.org.

Riaño, D., F. Valladares, S. Condés, and E. Chuvieco, 2004. Estimation of Leaf Area Index and Covered Ground From Airborne Laser Scanner (Lidar) in Two Contrasting Forests. Agricultural and Forest Meteorology 124:269-275.

Rueda, C.A., J.A. Greenberg, and S.L. Ustin, 2005. StarSpan: A Tool for Fast Selective Pixel Extraction From Remotely Sensed Data. Center for Spatial Technologies and Remote Sensing (CSTARS), University of California at Davis, Davis, California.

Ruiz-Arias, J.A., J. Tovar-Pescador, D. Pozo-Vazquez, and H Alsamamra, 2009. A Comparative Analysis of DEM-Based Models to Estimate the Solar Radiation in Mountainous Terrain. International Journal of Geographical Information Science 23(8):1049-1076.

Rutherford, J.C., S. Blackett, C. Blackett, L. Saito, and R.J. Davies-Colley, 1997. Predicting the Effects of Shade on Water Temperature in Small Streams. New Zealand Journal of Marine and Freshwater Research 31:707-721.

Soininen, A., 2004. TerraScan User's Guide. Terrasolid, Helsinki, Finland, 158 pp.

Šúri, M., and J. Hofierka, 2004. A New GIS-Based Solar Radiation Model and Its Application for Photovoltaic Assessments. Transactions in GIS 8(2):175-190.

Šúri, M., T.A. Huld, and E.D. Dunlop, 2005. PV-GIS: A Web-Based Solar Radiation Database for the Calculation of PV Potential in Europe. International Journal of Sustainable Energy 24(2):55-67.

U.S. Army Corps of Engineers, 2009. Engineering and Design: Guidelines for Landscape Planting and Vegetation Management at Levees, Floodwalls, Embankment Dams, and Appurtenant Structures. Department of the Army, U.S, Army Corps Engineers, Washington, D.C.

Webb, B.W., D.M. Hannah, R.D. Moore, L.E. Brown, and F. Nobilis, 2008. Recent Advances in Stream and River Temperature Research. Hydrological Processes 22(7):902-918.

Welty, J.J., T. Beechie, K. Sullivan, D.M. Hyink, R.E. Bilby, C. Andrus, and G. Pess, 2002. Riparian Aquatic Interaction Simulator (RAIS): A Model of Riparian Forest Dynamics for the Generation of Large Woody Debris and Shade. Forest Ecology and Management 162:299-318.

Widlowski, J.L., M. Taberner, B. Pinty, V. Bruniquel-Pinel, M. Disney, R. Fernandes, J.P. Gastellu-Etchegorry, N. Gobron, A. Kuusk, and T. Lavergne, 2007. The Third Radiation Transfer Model Intercomparison (RAMI) Exercise: Documenting Progress in Canopy Reflectance Models. Journal of Geophysical Research 112(D09111):1-28. http://www.agu.org/journals/jd/jd0709/2006JD007821/2006JD007821.pdf.